



OPEN ACCESS

EDITED BY

Chen Yang,
University of Chinese Academy of
Sciences, China

REVIEWED BY

Zhiwei Fang,
Johns Hopkins University, United States
Sneh Gautam,
G. B. Pant University of Agriculture and
Technology, India
Adeleh Gholipour-Kanani,
Islamic Azad University, Iran

*CORRESPONDENCE

Mantas Malinauskas,
mantas.malinauskas@ismuni.lt

SPECIALTY SECTION

This article was submitted to
Biomaterials,
a section of the journal
Frontiers in Bioengineering and
Biotechnology

RECEIVED 16 June 2022

ACCEPTED 19 July 2022

PUBLISHED 23 August 2022

CITATION

Malinauskas M, Jankauskaite L,
Aukstikalne L, Dabasinskaite L,
Rimkunas A, Mickevicius T,
Pockevicius A, Krugly E,
Martuzevicius D, Ciuzas D,
Baniukaitiene O and Usas A (2022),
Cartilage regeneration using improved
surface electrospun bilayer
polycaprolactone scaffolds loaded with
transforming growth factor-beta 3 and
rabbit muscle-derived stem cells.
Front. Bioeng. Biotechnol. 10:971294.
doi: 10.3389/fbioe.2022.971294

COPYRIGHT

© 2022 Malinauskas, Jankauskaite,
Aukstikalne, Dabasinskaite, Rimkunas,
Mickevicius, Pockevicius, Krugly,
Martuzevicius, Ciuzas, Baniukaitiene
and Usas. This is an open-access article
distributed under the terms of the
[Creative Commons Attribution License
\(CC BY\)](https://creativecommons.org/licenses/by/4.0/). The use, distribution or
reproduction in other forums is
permitted, provided the original
author(s) and the copyright owner(s) are
credited and that the original
publication in this journal is cited, in
accordance with accepted academic
practice. No use, distribution or
reproduction is permitted which does
not comply with these terms.

Cartilage regeneration using improved surface electrospun bilayer polycaprolactone scaffolds loaded with transforming growth factor-beta 3 and rabbit muscle-derived stem cells

Mantas Malinauskas^{1*}, Lina Jankauskaite¹, Lauryna Aukstikalne¹,
Lauryna Dabasinskaite², Augustinas Rimkunas¹,
Tomas Mickevicius¹, Alius Pockevicius³, Edvinas Krugly²,
Dainius Martuzevicius², Darius Ciuzas², Odeta Baniukaitiene²
and Arvydas Usas¹

¹Institute of Physiology and Pharmacology, Lithuanian University of Health Sciences, Kaunas, Lithuania, ²Faculty of Chemical Technology, Kaunas University of Technology, Kaunas, Lithuania, ³Department of Veterinary Pathobiology, Veterinary Academy, Lithuanian University of Health Sciences, Kaunas, Lithuania

Polycaprolactone (PCL) has recently received significant attention due to its mechanical strength, low immunogenicity, elasticity, and biodegradability. Therefore, it is perfectly suitable for cartilage tissue engineering. PCL is relatively hydrophobic in nature, so its hydrophilicity needs to be enhanced before its use in scaffolding. In our study, first, we aimed to improve the hydrophilicity properties after the network of the bilayer scaffold was formed by electrospinning. Electrospun bilayer PCL scaffolds were treated with ozone and further loaded with transforming growth factor-beta 3 (TGFβ3). *In vitro* studies were performed to determine the rabbit muscle-derived stem cells' (rMDSCs) potential to differentiate into chondrocytes after the cells were seeded onto the scaffolds. Statistically significant results indicated that ozonated (O) scaffolds create a better environment for rMDSCs because collagen-II (Coll2) concentrations at day 21 were higher than non-ozonated (NO) scaffolds. In *in vivo* studies, we aimed to determine the cartilage regeneration outcomes by macroscopical and microscopical/histological evaluations at 3- and 6-month time-points. The Oswestry Arthroscopy Score (OAS) was the highest at both mentioned time-points using the scaffold loaded with TGFβ3 and rMDSCs. Evaluation of cartilage electromechanical quantitative parameters (QPs) showed significantly better results in cell-treated scaffolds at both 3 and 6 months. Safranin O staining indicated similar results as in macroscopical evaluations—cell-treated scaffolds revealed greater staining with safranin, although an empty defect also showed better results than non-cell-treated scaffolds. The scaffold with chondrocytes

represented the best score when the scaffolds were evaluated with the Mankin histological grading scale. However, as in previous *in vivo* evaluations, cell-treated scaffolds showed better results than non-cell-treated scaffolds. In conclusion, we have investigated that an ozone-treated scaffold containing TGF β 3 with rMDSC is a proper combination and could be a promising scaffold for cartilage regeneration.

KEYWORDS

cartilage regeneration, PCL scaffolds, ozone treatment, transforming growth factor-beta 3, rabbit MDSCs, cell-scaffold construct

1 Introduction

The subsequent healing of articular cartilage remains a significant clinical problem. Adult human articular cartilage is approximately 2–4 mm and serves as a cushion for joints against a physiological load (Hunziker et al., 2002). Because cartilage lacks nerves, blood vessels, and lymphatics, its ability to regenerate itself is restricted (Li et al., 2022). Thus, cartilage degradation can quickly lead to gradual tissue deterioration, persistent joint pain, dysfunction, and finally to the degenerative disease, osteoarthritis (OA) (Borrelli et al., 2019). To protect the cartilage from further degradation, it is necessary to apply the appropriate treatment. For many years, orthopedic surgeons treating articular cartilage injuries sought to achieve stable fixation of the articular cartilage surface restoration of limb alignment and joint stability (Borrelli et al., 2019). However, such treatment is not fully effective in cartilage preservation as it is also important to emphasize that there is an ongoing cellular response that needs to be controlled (Li et al., 2022). Following initial cartilage damage, local cells release inflammatory factors into the synovial fluid, which surrounds the cartilage (Sokolove and Lepus, 2013). These inflammatory factors, such as interleukin-1 or/and 6 (IL-1, IL-6), and tumor necrosis factor-alpha (TNF- α) inhibit chondrogenesis (Choukair et al., 2014). To improve neo-tissue formation, the impact of inflammation on cartilage tissue should be considered. A variety of techniques exist in articular cartilage repair and regeneration, each with its own advantages and drawbacks (Makris et al., 2015). The microfracture technique has limitations in chondrogenesis as this technique results in fibrocartilage formation, that is, biochemically and biomechanically inadequate for hyaline articular cartilage (Bae et al., 2006). Tissue engineering approaches using a variety of cell sources including autologous, allogenic, and xenogeneic stem cells have resulted in the repair of tissues with hyaline-like properties (Jelodari et al., 2022). Cartilage engineering by embedding relevant cells like articular chondrocytes or mesenchymal stem cells (MSCs) and growth factors, particularly transforming growth factor beta (TGF β) (Wang et al., 2014), into scaffolds support chondrocyte growth and proliferation (Francis et al., 2018). In addition, MSCs scaffolding together with loaded differentiation factors, TGF β 1 or TGF β 3, may enhance articular cartilage formation because of their anti-

inflammatory potential (Yoshimura et al., 2010; Stewart et al., 2018). MSCs are multipotent progenitor cells that can self-renew and differentiate into cartilage (Gomez-Salazar et al., 2020), while the most commonly used adult source tissue for human MSCs are bone marrow, muscle, and adipose tissue (Pittenger et al., 2019). Muscle-derived stem cells (MDSCs) have clonogenicity and growth kinetics superior to bone-derived stem cells (Čamernik et al., 2019). The necessity for a biomaterial scaffold to stimulate cell attachment, spreading, migration, proliferation, and differentiation for successful tissue regeneration is a fundamental challenge in tissue engineering in 3D microenvironments (Mohammadinejad et al., 2020). Biomaterials should be biodegradable and should have the same mechanical properties as native cartilage. However, no single best material is available that would be the gold standard for tissue engineering. Polycaprolactone (PCL) has recently received significant attention due to its mechanical strength, low immunogenicity, elasticity, biodegradability, and biocompatibility (Theodoridis et al., 2019). PCL scaffolds can promote stem cell differentiation and proliferation, while their hydrophobic profile inhibits cellular attachment, limiting their suitability in tissue engineering (Sousa et al., 2014). However, the surface of porous 3D PCL scaffold modification improves the hydrophilic properties and growth factor release (Qin et al., 2022). Treatment with ultraviolet irradiation and ozone (O₃) increases the surface hydrophilicity of PCL scaffolds for effective cell attachment and proliferation (Samsudin et al., 2017).

In this study, we aimed to evaluate the formation of cartilage tissue using rabbit muscle-derived stem cells (rMDSCs) on electrospun bilayer PCL ozone-treated scaffolds with loaded TGF β 3. The latter has been developed and validated *in vitro* during our earlier investigations (Dabasinskaite et al., 2022; Jankauskaite et al., 2022). First, we investigated the scaffold's potential *in vitro* to provide and maintain a microenvironment for rMDSC proliferation and differentiation into chondrocytes. In addition, to elucidate the advantages of ozone-treated (O) over non-ozonated (NO) scaffolds in order to select a more suitable scaffold variant for *in vivo* studies, we hypothesized that PCL ozone-treated scaffolds with loaded TGF β 3 and rMDSCs would outperform other groups and will show similar results to the control group—scaffolds with chondrocytes in the *in vivo* rabbit model for supporting neocartilage formation. Such

demonstration of this type of scaffold has not been described earlier.

2 Materials and methods

2.1 Polycaprolactone scaffold characteristics

The scaffold was formed from a two-layer composite of fibrous matrixes, each having variations in composition and processing. The chondral layer polymer solution was composed of poly(ϵ)caprolactone (PCL, IUPAC name: (Hunziker et al., 2002; Bae et al., 2006)-polyoxepan-2-one, CAS: 24980-41-4, Mn—80 kDa, Cat. No: 440744) dissolved with cellulose and cellulose acetate (CA, 39.7% acetyl content, Mn—50 kDa, CAS: 9004-35-7). The subchondral layer polymer solution was prepared similarly to the chondral layer, except that hydroxyapatite (HA, <15 μ m particle size, CAS: 1306-06-5) powder was added. The fabrication procedure of both layers and electrospinning and ozonation techniques (treatment with O₃) were described previously (Dabasinskaite et al., 2021; Dabasinskaite et al., 2022). PCL pellets and CA powder (2:1, w/w) were dissolved in acetone and N,N-dimethylformamide mixture at 2:3 (v/v) to obtain 30% (w/v) polymer solution. The mixing process was carried out at 40°C on the magnetic stirrer. The scaffolds were fabricated by using a cryo-electrospinning setup (voltage 26–28 kV, temperature 35°C, and RH 30%). The scaffolds were post-treated to convert cellulose acetate to cellulose and to introduce functional groups for the binding of the growth factor. The fabricated fibrous mats were cut into scaffold specimens (6 mm in diameter and a weight of 0.50 g). The scaffolds were placed in a glass reactor containing water (20°C) and treated by bubbling O₃ from an *ex situ* generator into the reactor at a mass flow of 400 mg/h. Subsequently, the samples were stored in a vacuum dryer at 21°C for 12 h. Before *in vitro* and *in vivo* experiments, scaffolds were sterilized with ethylene oxide. The scaffold was cut into 6 mm diameter and 1 mm height sample discs for *in vitro* and *in vivo* studies.

2.2 Transforming growth factor-beta 3 loading on bilayer polycaprolactone scaffolds

Dosage and timing of TGF β 3 (Thermo Fisher Scientific, United States) loading on PCL were selected, as previously described (Jankauskaite et al., 2022). In brief, scaffolds were incubated with 10 ng/ml TGF β 3. After the most efficient binding duration was clarified, samples for *in vitro* and *in vivo* experiments were covered with 100 μ l of 10 ng/ml TGF β 3 for 24 h, providing sufficient time for protein binding to unmodified and modified scaffolds (Dabasinskaite et al., 2022).

Subsequently, the unbound protein was washed with PBS, and scaffolds were submitted for further experiments.

2.3 Ethics in animal experimentation

Tissue collection for rMDSC and rabbit chondrocyte (rCh) isolation and further *in vivo* studies in rabbits were approved by the Ethics Committee of the State Food and Veterinary Service (No G2-133).

2.4 Isolation, differentiation, and characterization of rabbit muscle-derived stem cells

Biopsies of skeletal muscles of New Zealand rabbits ($n = 4$) were collected, and rMDSCs were isolated using a pre-plating technique with some modifications (Lavasani et al., 2013). After washing, dissecting from residual tendon, fat, and connective tissue, and mechanical digestion, minced muscle tissue was submitted for enzymatic digestion with 0.2% of collagenase type XI and kept with gentle continuous rocking at 37°C for 1.5 h. Furthermore, the previously described protocol was followed with an adjusted centrifugation speed of 1,400 rpm for 5 min (Lavasani et al., 2013). Obtained cells were cultivated in a monolayer on the collagen-coated surface using Dulbecco's modified Eagle's medium (DMEM) with 4.5 g glucose/L (Gibco, United Kingdom), supplemented with 10% fetal bovine serum (FBS) (Gibco, United Kingdom), 10% horse serum (HS) (Gibco, United Kingdom), 0.5% chicken embryo extract (LSP, United Kingdom), and 1% penicillin/streptomycin [Penicillin/Streptomycin (10000 U/l) (P/S), Gibco, United Kingdom] at 37°C in a 5% CO₂ humidified incubator. The medium for rMDSCs was changed every 3 days. Passages 5 up to 10 were used for further experiments.

First, the morphology of cells was evaluated *via* light microscopy. The lineage of isolated rMDSCs was identified by flow cytometry for strain biomarkers and by differentiation ability. Also, the sixth passage of rMDSCs was tested for CD45, CD44, and CD105 (Invitrogen, United States) by flow cytometry [FACSMelody (BD)]. Multipotent differentiation capacity was proven by induced, adipogenic, osteogenic, and myogenic differentiation in a monolayer and chondrogenic differentiation in pellet culture. Adipogenesis was induced with an adipogenesis differentiation medium (Gibco, United Kingdom). After 14 days of cultivation, adipogenic cultures were stained with Oil Red O (Sigma-Aldrich, United States) for microscopic visualization of lipid droplets. Osteogenesis was evaluated *via* microscopy when cultures were stained with alizarin red (Sigma-Aldrich, United States) and after 14 days of incubation with an osteogenesis differentiation medium (Gibco, United Kingdom). The chondrogenic

capacity was proved by successful chondrogenic pellet formation after 21 days of incubation with chondrogenesis differentiation medium (Gibco, United Kingdom) and stained with safranin O (Sigma-Aldrich, United States) and toluidine blue (Sigma-Aldrich, United States). Myogenesis was analyzed by muscle-specific desmin protein detection with immunohistochemistry using rabbit anti-desmin antibodies (Sigma-Aldrich, United States), and cell nuclei were highlighted by DAPI fluoroshield (Sigma-Aldrich, United States).

After differentiation, rMDSCs were fixed with 1% PFA and stained, as previously described. Fixed differentiated rMDSCs were evaluated *via* microscopy (Olympus BX63, Japan).

2.5 Isolation and monoculture of rabbit chondrocytes

Each biopsy sample of rabbit articular cartilage was taken from the intercondylar notch and immersed in a 50-ml conical sterile polypropylene centrifuge tube (TPP, Switzerland) containing a total of 15 ml transport medium with 12 ml of DMEM, 3 ml of fetal bovine serum (FBS) (Gibco, United Kingdom), and 15 μ l of 0.1% gentamycin (Gibco, United Kingdom). The biopsy was transported immediately to the laboratory for further chondrocyte isolation procedure. The sample of articular cartilage was three times washed with Hams/F12 (Gibco, United Kingdom) containing 1% penicillin/streptomycin [penicillin/streptomycin (10000 U/l), Gibco, United Kingdom]. The cartilage was then minced with a sterile scalpel blade into small pieces in a petri dish containing 2 ml of protease (type XIV, >3.5 U/mg, Sigma-Aldrich, United States) solution. The minced cartilage was transferred into the tube with 8 ml of protease solution and left for digestion for 60 min at 37°C, with 5% CO₂. After 60 min, the protease solution was changed to 10 ml of collagenase (type A > 150 U/mg, Worthington Biochemical, United States) solution, and cartilage pieces were digested for 16 h at 37°C and 5% CO₂. The enzymatic reaction was neutralized with 10 ml of DMEM supplemented with 10% FBS and 0.1% gentamycin (medium) and then filtered through a 70- μ m cell strainer (Falcon, United Kingdom) into a 50-ml tube and centrifuged at \times 300 g (4°C) for 10 min. The supernatant was carefully discarded, and the cell pellet was filled with a fresh 1 ml of medium. The mixture was resuspended, and the cell count and viability were determined by the trypan blue dye exclusion test. The cells were plated in tissue culture flasks at a density of 2×10^3 cell/cm². The morphology of the cells was examined regularly, and the image was taken with a microscope. When the cells reached 80%–90% confluence, they were trypsinized by TrypLE-Express enzyme (x1) and phenol red (Gibco, United Kingdom), and chondrocytes [passage 0 (P0)] were harvested, centrifuged, and resuspended in a culture medium. The culture medium was changed every 3 days. Cells were replated at a density of $2\text{--}6 \times 10^3$ cm².

2.6 Pellet culture

rMDSC and rCh pellets were established in microcentrifuge tubes by suspension of 2×10^5 cells in 400 μ l of the medium. The tubes were centrifuged at \times 300 g (4°C) for 6 min. The tops of the tubes were perforated with an 18-gauge needle after centrifugation to permit gaseous exchange. After 72 h, corresponding to the first time, the medium was changed, and the pellets were gently detached from the bottom. This procedure was repeated every 3 days until the 21-day pellet-culturing time-point was reached. The rMDSC pellet was cultured in a chondrogenesis differentiation medium (Gibco, United Kingdom). Control pellets containing rMDSC cells were cultured using an identical cell culture medium described in Section 2.5. The triplets of both pellets including rMDSC and control were formed.

2.7 Cell proliferation assay

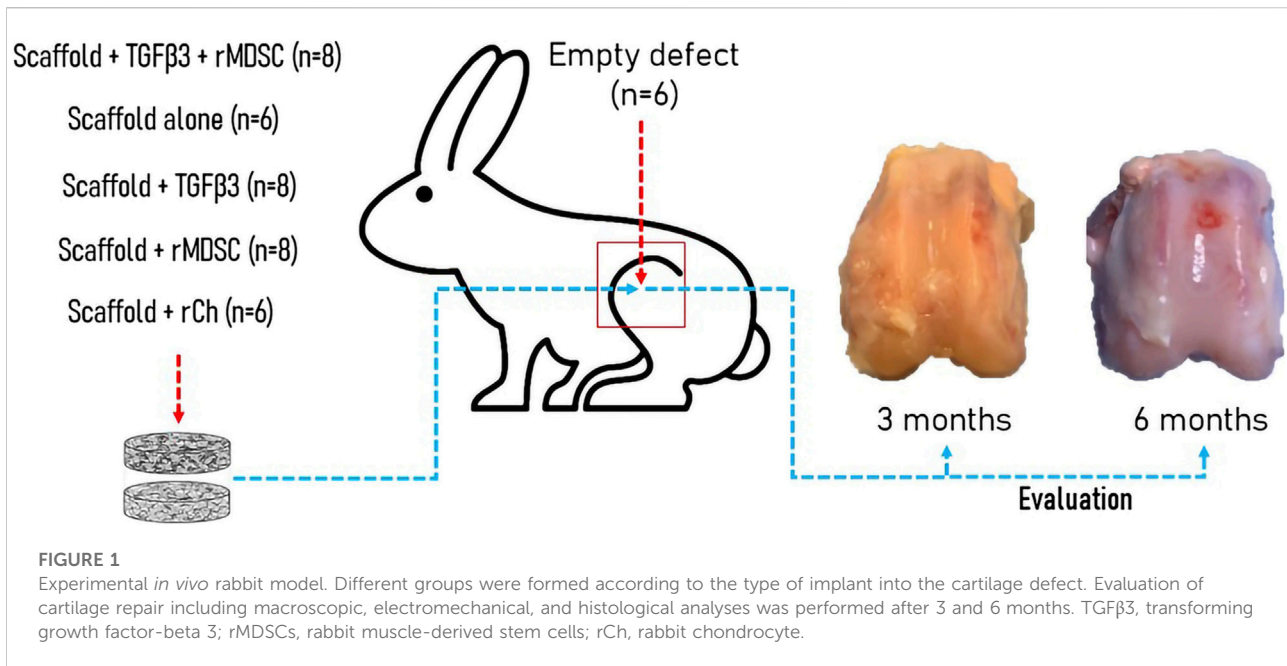
Unstained cell-scaffold complexes were cultivated in 96-well plates. Briefly, cells were seeded on scaffolds at a density of 50,000 cells per scaffold. Three replicates were set up for each group. Cell proliferation was examined at the following time-points: days 1, 3, 7, 14, and 21. On each day, 10 μ l of the CCK-8 (Abcam, United States) solution was added to each well with the cell-scaffold complex. After 3–4 h incubation, the medium was collected into separate 96-well plates, and the absorbance of each well was measured using a microplate reader (Thermo Fisher Scientific, Finland).

2.8 Enzyme-linked immunosorbent assay

TGF β 3 and collagen 2 (Coll2) concentrations in the supernatants during culturing were quantified using ELISA kits. The cell culture medium from TGF β 3-loaded NO or O scaffolds and non-TGF β 3-loaded NO or O scaffolds, both rMDSC and hCh were aspirated on days 1, 3, 7, 14, 21, and 28, frozen at -80°C , and kept until needed (less than one month). TGF β 3 and Coll2 were measured according to the protocols of commercially available ELISA kits: TGF β 3 (Assay Biotech, United States) and Coll2 (Cloud-Clone Corp., United States). Absorption at 450 nm was measured using a microplate reader (Multiskan GO 1.00.40 (Thermo Fisher Scientific)).

2.9 Animal surgery and scaffold preparation

Twenty-three male 3–4-month-old New-Zeeland White rabbits were used for the study. Each knee was randomly assigned to one of the following treatment groups. There were



six experimental groups according to the treatment and bilayer scaffold preparation for implantation into cartilage defect (Figure 1). There were the following groups: empty defect (E, $n = 6$), scaffold alone (cell-free and growth factor free) (S, $n = 6$), TGFβ3-loaded scaffold (St, $n = 8$), TGFβ3-loaded scaffold + rMDSC (Stm, $n = 8$), scaffold with rMDSC (Sm, $n = 8$), and scaffold with rabbit chondrocyte (rCh) (Sc, $n = 6$) groups. Ozonated scaffolds were used in all groups. Rabbits were euthanized 3 and 6 months after surgery. Two animals did not survive until the end of the designated time-point and were excluded from the study.

2.10 Surgical procedure

Under general isoflurane (Vetpharma Animal Health, Barcelona, Spain) anesthesia, following shaving and sterile preparation of both legs, a 3-cm medial parapatellar incision was made in each knee, exposing the patellofemoral groove. Using slow-speed dental trephine under constant irrigation with saline, an osteochondral defect, measuring 4.5 mm in diameter and 4–5 mm deep, was created in a trochlear groove in both knees. Defects were filled with a two-layer scaffold that consisted of the chondral layer made of poly(*e*)caprolactone and cellulose (PCL-CEL) at the top prepared in different ways and the subchondral layer made of PCL-CEL-HA at the bottom. Scaffolds were press-fitted into the cartilage defect and sealed with fibrin glue (Tisseel Lyo, Baxter, Switzerland). Following wound closure, the knee was moved through a full range of motion to ensure normal patellar tracking. After surgery, all

animals were allowed to move freely in the cages and provided with food and water *ad libitum*.

2.11 Macroscopic evaluation and grading of the cartilage repair site

Thereafter, 3 and 6 months after implantation, animals were euthanized, and the articular cartilage defect repair site was evaluated macroscopically and assessed using a modified Oswestry Arthroscopy Score (OAS) by two independent researchers. According to this scoring system, the score was based on a point system with a total of 8 points, representing healthy cartilage. Repair tissue surface level, integration with surrounding cartilage, appearance, and color of the repair tissue surface were assessed. Stiffness on probing was excluded in our study because repaired cartilage properties were evaluated electromechanically by using an Arthro-BST device (Biomomentum Inc., Laval, Quebec, Canada).

2.12 Electromechanical evaluation

Electromechanical properties of cartilage were evaluated using an Arthro-BST device 3 and 6 months after transplantation, as described elsewhere (Mickevicius et al., 2015). Briefly, positively charged mobile ions in the cartilage stroma are displaced, with respect to the fixed and negatively charged proteoglycan molecules during cartilage compression. The probe of the device registers streaming potentials after

compression, and with the assistance of software, it generates quantitative parameters (QPs) in numeric values from 0 to 36. The high QP parameter is a digital reflection of extracellular matrix disintegration, weak electromechanical properties, and inferior load-bearing capacity of the cartilage, while low QP indicates strong electromechanical properties and superior load-bearing capacity. QP measurements in each repair site were recorded four to five times to obtain median values.

2.13 Histological evaluation and grading

After macroscopic and QP examination, distal femurs of the rabbits were dissected, fixed in 10% neutral buffered formalin, decalcified, and embedded in paraffin. Then, 5-F06DM thick sagittal sections were stained with safranin O/fast green, as previously described (Mickevicius et al., 2015). Light microscopy images of the repair site were taken at x 40 magnification with an Olympus BX61 microscope equipped with an Olympus DP72 CCD camera by cellSens Dimension imaging software (Olympus, Japan). A total of 30 snap pictures of the entire implantation site were combined into one final picture using the manual stitched image acquisition function of the software. The quality of the repaired cartilage was blindly evaluated by two investigators using the Mankin histological grading score, as described in Pearson et al. (2011). According to the Mankin grading system, healthy cartilage is rated with 0 points. The articular surface is rated 0–4 from smooth to cracked or completely disorganized, respectively. Chondrocyte morphology and proliferation are assessed from 0 (normal cell distribution) to 3 points (zones without cells). The extent of safranin-O staining is assessed from 0 to 4 points (not stained). With a maximum of 11 points, the cartilage is estimated as fully damaged.

2.14 Statistical analysis

Statistical analysis was accomplished by IBM SPSS 28.0 software (SPSS Inc., Chicago, IL, United States) for Windows. All the quantitative data were expressed as mean \pm standard deviation (SD). Kruskal–Wallis and Mann–Whitney U tests were used to analyze the differences. A *p*-value of <0.05 was considered significant.

3 Results

3.1 Isolation, differentiation, and characterization of rabbit muscle-derived stem cells

Rabbit MDSCs were isolated from a few rabbits and analyzed by flow cytometry. FACS analysis showed the expressions of

rabbit stem cell surface markers (CD44 and CD105) and lack of the hematopoietic marker (CD45) on pp6 (Figure 2A). Isolated cells excelled by homogeneity and rapid proliferation after pre-plate 6 cells were expanded (Figure 2B). Pp6 cells demonstrated adipogenic differentiation capacity after 14 days of cultivation in an adipogenic induction medium (Figure 2C, adipogenesis). The myogenic potential was determined by finding desmin-positive cells after 18 days of incubation with a low-serum myogenic medium (Figure 2C, myogenesis). After 14 days, rabbit MDSCs differentiated into osteocytes, and after 21 days, they formed a chondrogenic pallet which stained positive for safranin and toluidine blue, as shown in Figure 2C.

3.2 Rabbit muscle-derived stem cell proliferation and differentiation into chondrocytes

At the initial time-points (D1–D7), there was a significantly lower proliferation rate of rMDSCs on NO scaffolds than NO loaded with TGF β 3, as well as O with or without a TGF β 3 ($p < 0.01$) (Figure 3A). On day 14, NO showed a significant increase in rMDSC growth compared to NO loaded with TGF β 3. However, there were no significant cell growth changes when compared to the other two scaffolds. We analyzed the TGF β 3 protein release but observed no difference between the NO and O scaffolds loaded with TGF β 3 ($p > 0.05$) (Figure 3B). In addition, untreated scaffolds were tested to assess if rMDSCs produced TGF β 3; however, no protein was identified (data not shown).

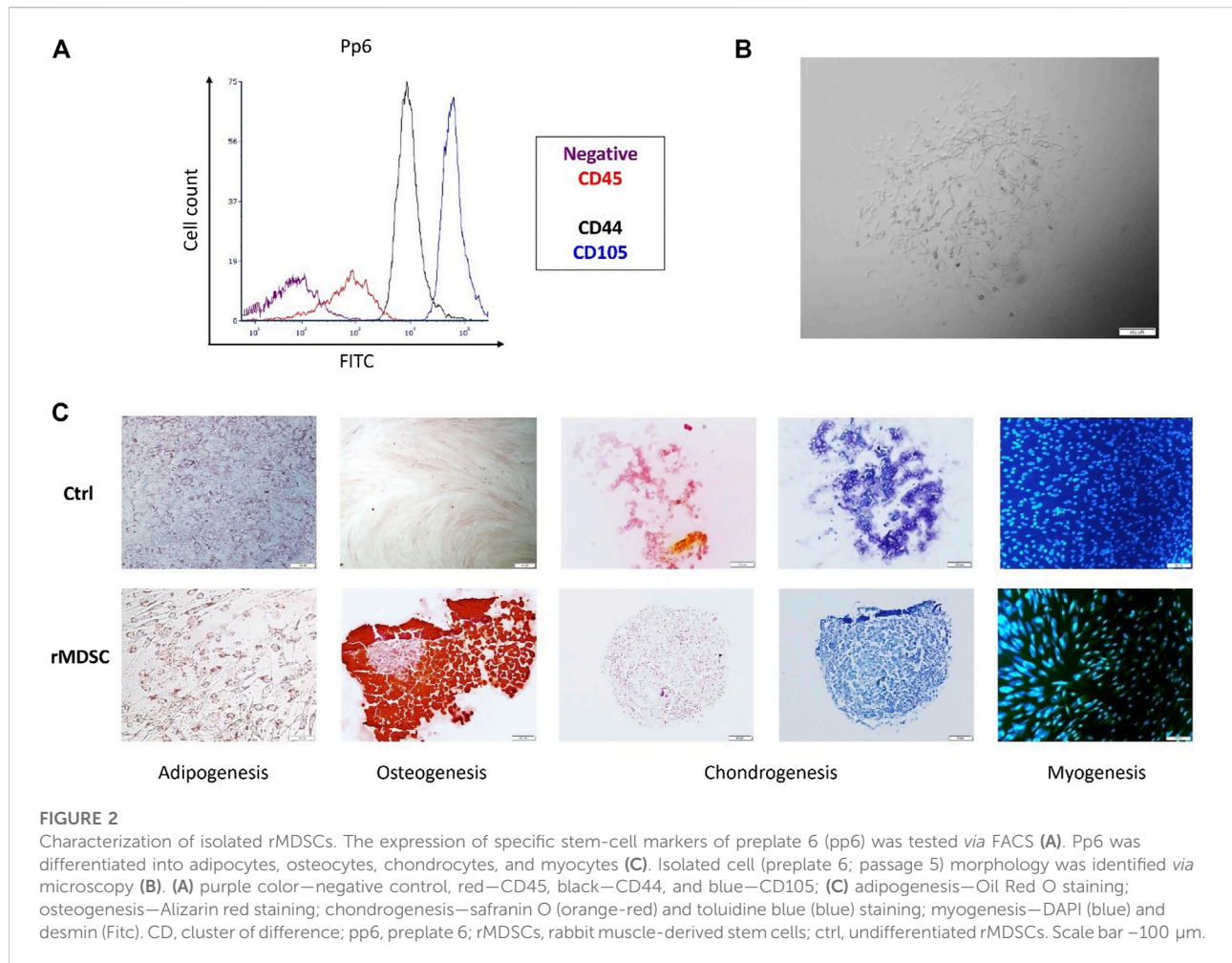
Nevertheless, on day 21, ozonated TGF β 3-loaded PCL scaffolds showed increased Coll2 production, suggesting rMDSC differentiation into chondrocytes ($p < 0.001$) (Figure 3C).

3.3 Macroscopic evaluation and grading of the cartilage repair site

Considering that ozonated scaffolds provided a better environment in our *in vitro* studies and based on our previous research (Jankauskaite et al., 2022), they were further submitted for *in vivo* experiments.

The macroscopic images of the rabbit femoral condyles at 3 and 6 months after transplantation are depicted in Figure 4A. The mean Oswestry Arthroscopy Score (OAS) values in each experimental group are shown in Figure 4B.

Stm and Sm demonstrated better results 3 months after transplantation (mean score— 7.50 ± 0.58 and 7.25 ± 0.5 , respectively). Stm and Sm had significantly higher scores than E, S, St, or Sc. Sc showed significantly higher scores (mean score 6.38 ± 0.63) than S but significantly lower scores than Stm and Sm. Overall, E, S, and St had lower scores (5.38 ± 1.38 , 4.88 ± 0.25 , and 5.38 ± 0.48 , respectively).



At 6 months post-transplantation, Stm scored a high score (7.0 ± 0.82), and Sm and Sc scores were significantly higher than E, S, and St, but no difference was found between these groups. Sc was superior to E, S, and St ($p < 0.05$) (Figure 4B).

Overall, during the period from 3 to 6 months, results tended to show slight macroscopic score deterioration. Defects filled with S and Sc had statistically lower scores at 6 months than at 3 months, while scores of E, St, Stm, and Sm were similar between the time-points.

3.4 Electromechanical evaluation

Greater electromechanical quantitative parameter (QP) values represent greater degenerative changes in the cartilage (Figure 4C). After 3 months post-transplantation, the highest QP values were observed in the empty defect ϵ and defect filled with scaffold alone (S) (10.85 ± 1.1 and 12.5 ± 3.87 , respectively) compared to defects filled with St, Stm, and Sc scaffolds which had significantly lower QP values $p < 0.05$. St-, Stm-, and Sm-treated groups revealed similar results to Sc. Overall, Stm

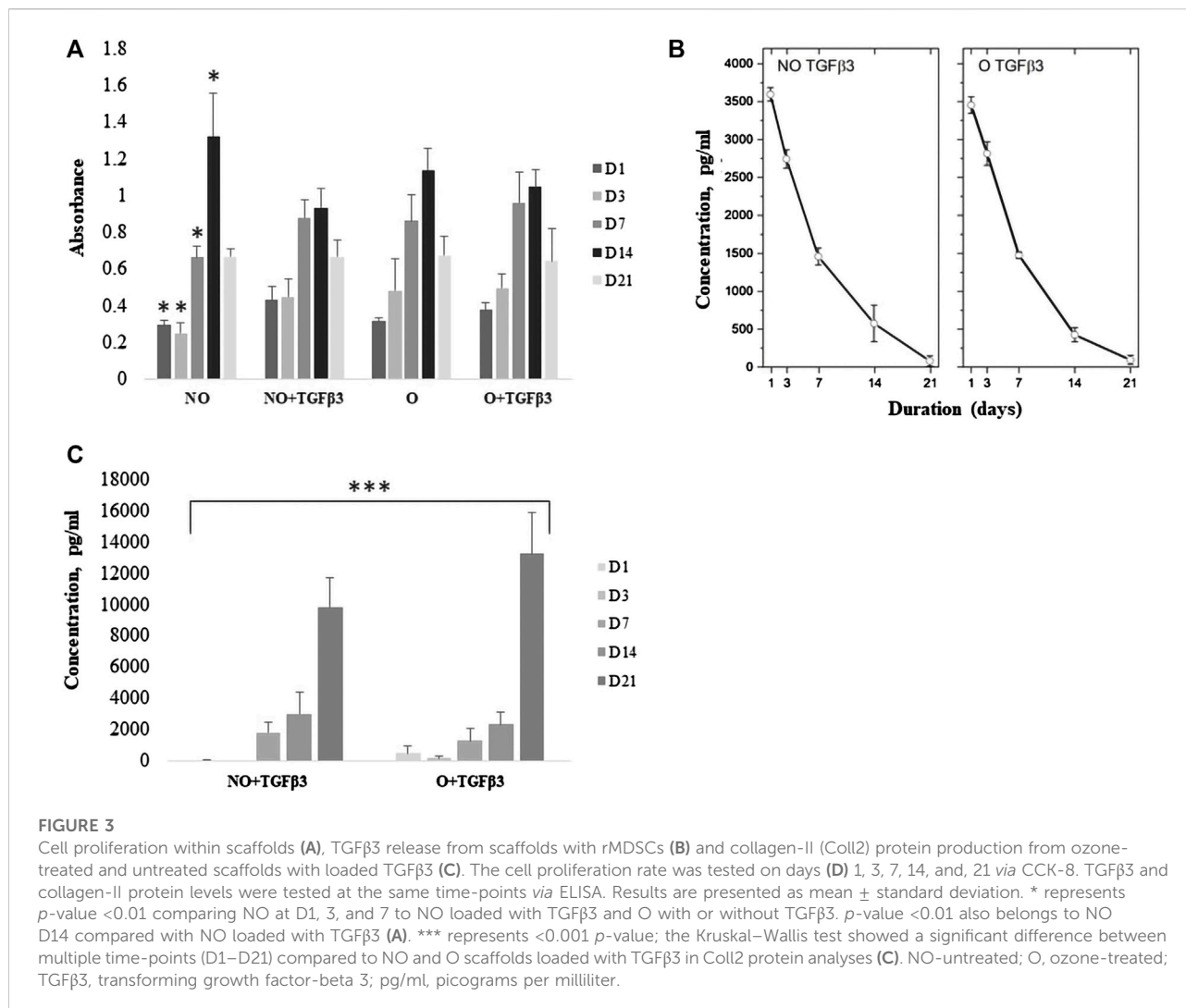
demonstrated the best QP value (5.95 ± 1.42); however, it was not significant compared to St, Sm, and Sc.

We observed similar tendencies 6 months post-transplantation. Worst QP values were registered in the E and S groups (14.15 ± 1.46 and 15.69 ± 1.46 , respectively). In contrast to 3 months, at 6 months post-transplantation, S and St had significantly worse results than scaffolds with cells ($p < 0.05$). The best electromechanical values were attributed to Stm- and Sc-treated groups (7.05 ± 1 and 7.30 ± 2.04 , respectively).

Comparing degenerative processes between 3 and 6 months post-transplantation, scaffolds without cells demonstrated clearly worse results than cellular scaffolds. The worst electromechanical measurements were found in empty defects and S scaffolds (Figure 4C). However, no statistical cartilage deterioration was observed in all cellular scaffolds after 6 months.

3.5 Histological evaluation and grading

Images of histological sections stained with safranin-O/fast green are presented in Figure 5A. Mankin histological grading



scores in each experimental group are summarized in Figure 5B. At 3 months postoperatively, the repaired tissue was consistently well organized in all groups. Membranes were partially bonded to the adjacent cartilage and the subchondral bone, and little clustering was detected at the border of native cartilage. Active integration with adjacent cartilage was less evident. All grafts exhibited hyaline cartilage morphology (scarcity of safranin-O staining). Sc scaffolds demonstrated the best results after 3 months (3.0 ± 0.41). Stm and Sm had similar scores and were significantly better than S and St scaffolds (4.25 ± 1.26 and 4.5 ± 0.58 , respectively). Interestingly, inferior results were observed in S (9.0 ± 1.83) and St scaffolds (7.25 ± 1.5) compared to cellular scaffolds ($p < 0.05$). Remarkably, empty defects had significantly better scores than S and St scaffolds and significantly worse scores than Sc scaffolds ($p < 0.05$), but no difference was observed with Stm and Sm scaffolds.

We observed similar results after 6 months. E, St, Stm, and Sm scores were similar. The worst results were observed in S and

St scaffold groups (10.63 ± 0.75 and 7.75 ± 1.5 , respectively), and it was clearly inferior to all other treatment groups ($p < 0.05$).

4 Discussion

With an increased life expectancy, there is an augmentation in degenerative conditions affecting cartilage tissue; thus, articular cartilage repair *via* different regenerative techniques is highly investigated. Recently, a focus has been set on engineering a biomimetic cellular microenvironment for the regeneration of a cartilaginous tissue, which has no potential to rejuvenate by itself. In our study, we aimed to examine the properties of an electrospun PCL bilayer scaffold consisting of a chondral layer with or without TGFβ3 and seeded with rMDS and a subchondral layer supplemented with HA. To the best of our knowledge, this is the first study demonstrating that the PCL scaffold created a proper microenvironment for rabbit MDSCs

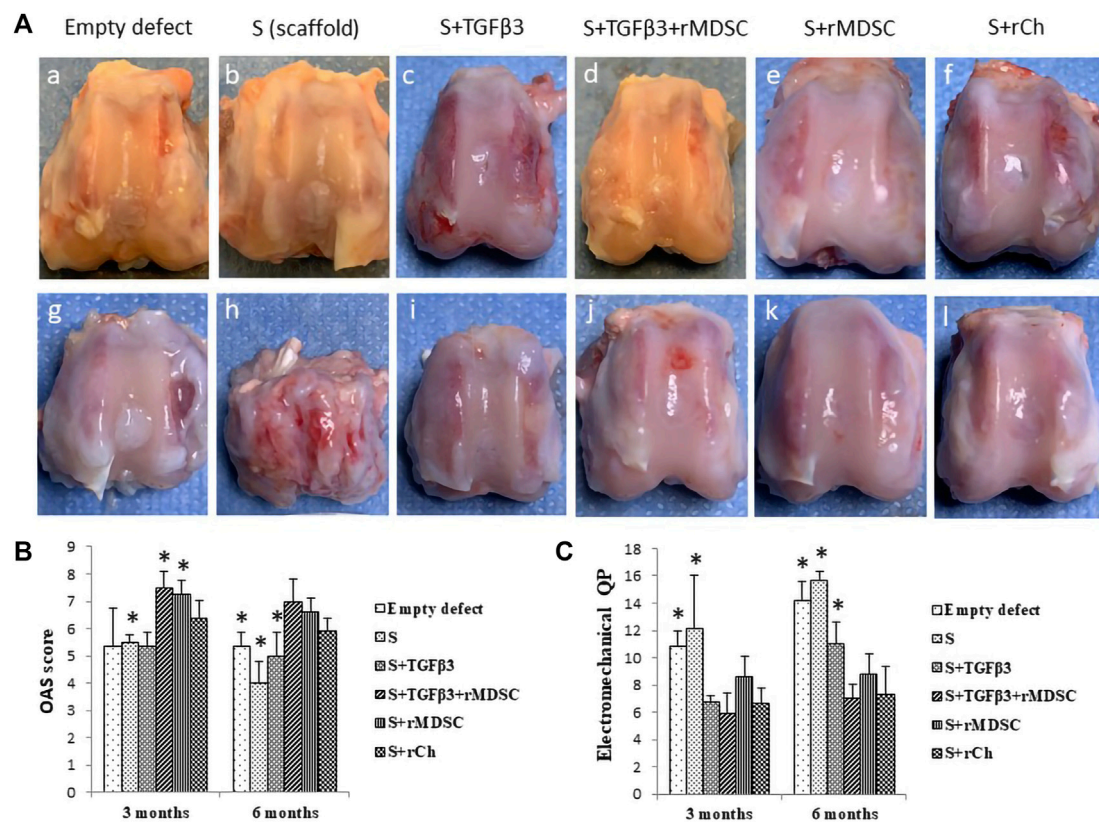


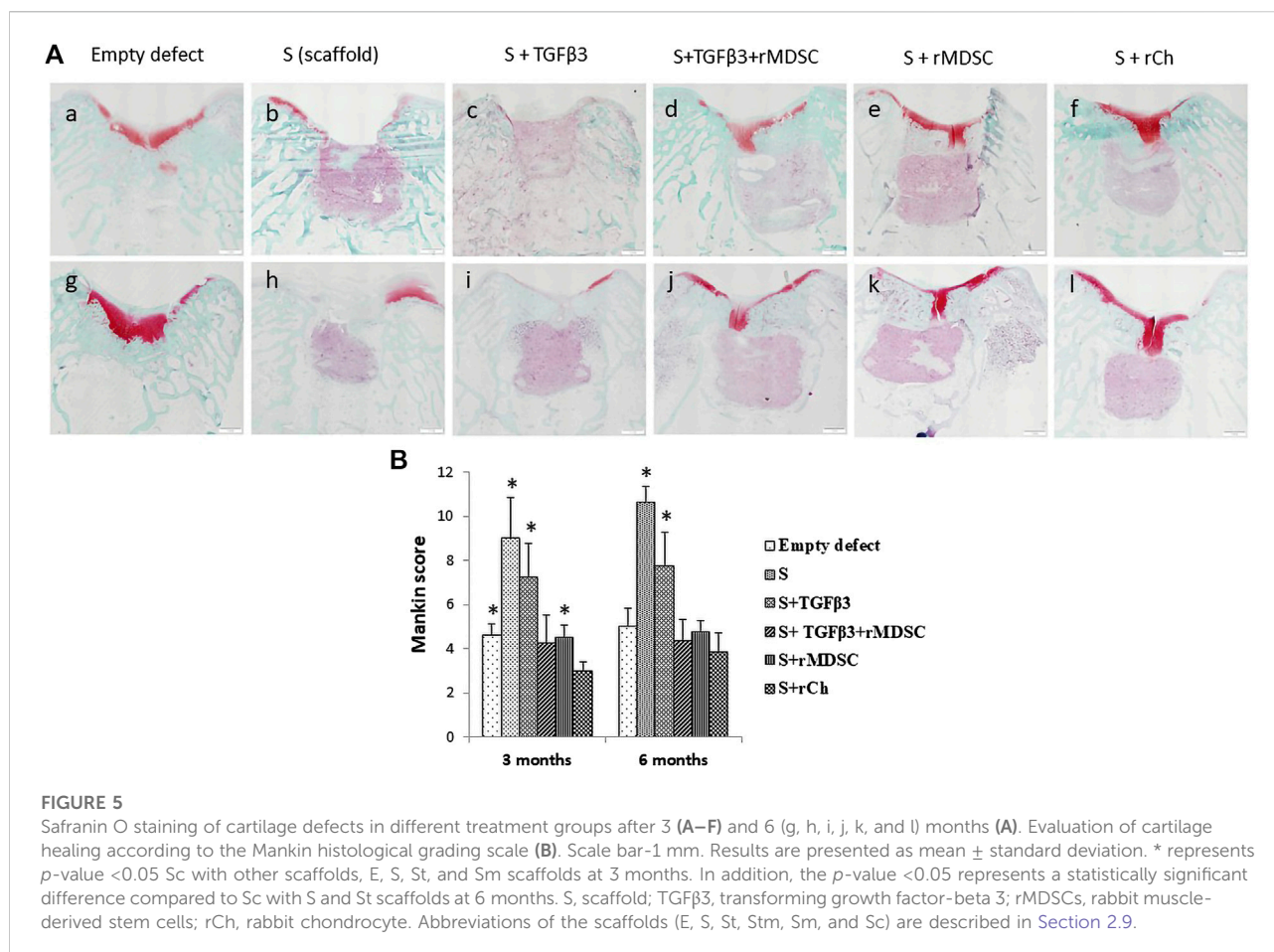
FIGURE 4

Healing of cartilage defects with different scaffolds after 3 (A–F) and 6 (g, h, i, j, k, and l) months (A). Macroscopic evaluation of cartilage defect healing according to the Oswestry Arthroscopy Score (OAS) (B). Evaluation of cartilage electromechanical quantitative parameters (QPs) by using the Arthro-BST device (C). Results are presented as mean \pm standard deviation. * represents p -value < 0.05 compared to Sc with other scaffolds—S, Stm, and Sm at 3 months. In addition, the p -value < 0.05 represents the difference compared to Sc with E, S, and St at 6 months (B). p -value < 0.05 showed as * indicates significant differences between Sc and E or S scaffolds at 3 months, also comparing Sc with E, S, and St scaffolds at 6 months (C). S, scaffold; TGF β 3, transforming growth factor-beta 3; rMDSCs, rabbit muscle-derived stem cells; rCh, rabbit chondrocyte. Abbreviations of the scaffolds (E, S, St, Stm, Sm, and Sc) are described in Section 2.9.

and showed highly promising results toward neocartilage formation *in vitro* and *in vivo*.

Cells and their microenvironment are highly important in the regenerative process. First, such elements as chemical properties, technical composition, and mechanics are associated with cell behavior, e.g., their migration, proliferation, or differentiation (Demoor et al., 2014; Girão et al., 2020; Abpeikar et al., 2021). For our scaffold production, we selected PCL, a highly biodegradable, elastic, and low cytotoxic material used in the electrospinning process, which provided a porous structure for our scaffolds. The porosity of the chondral layer was 90.7%; the mean pore diameter was 171 μ m. For the subchondral layer, porosity was 94.4%, and the mean pore diameter was 240 μ m. To improve its properties, scaffolds underwent ozone treatment and were further modified by supplementation of TGF β 3 protein. Ozone treatment has been already analyzed and shown to impact cell adhesion and proliferation (Redigueri et al., 2017;

Samsudin et al., 2018). In addition, this process can improve attachment of growth factors such as insulin growth factor-1 (Dabasinskaite et al., 2021) necessary to increase required differentiation toward chondrocytes, while the present study did not show an obvious impact on better TGF β 3 attachment than non-ozonated scaffolds. As we used rMDSCs, we selected TGF β 3 as the additional factor which is a confirmed factor in stimulating stem cells to undergo the chondrogenesis process (Grafe et al., 2018; Music et al., 2020). This material and technique already examined in different studies created a proper environment for our cells—rabbit MDSCs and chondrocytes. We did show its potential in the previous experimental study as well (Jankauskaite et al., 2022). The proliferation capacity was increased within the first 14 days. Ozonation and protein loading gave clear advancement as rMDSCs proliferated significantly more in three scaffolds (NO + TGF β 3, O, and O + TGF β 3) and provided a superior environment for the cells. Even though we could not detect



differences in TGFβ3 amounts between NO and O loaded with protein, ozone-treated protein-loaded PCL scaffolds demonstrated to provide a superior environment regarding neocartilage formation *in vitro*. The environment influencing and inducing proliferation is important, but differentiation toward chondrocytes is obligatory. Our scaffolds met those two requirements; moreover, cells were viable for 21 days, and differentiation into chondrocytes was observed starting on day 7. Interestingly, ozonated scaffolds loaded with TGFβ3 stimulated chondrogenesis earlier—starting on day 1 (after seeding).

At 3 months, the histological defect filled with the scaffold loaded with TGFβ3 and seeded with rMDSC had statistically comparable regeneration to the control group—the scaffold with chondrocytes. When scaffold-containing rMDSC was compared to a scaffold loaded with TGFβ3, the previous scaffold showed better regeneration. It suggests that rMDSCs, in the presence of TGFβ3, provide superior conditions for cartilage regeneration than using scaffolds only with cells. The positive effect of TGFβ3 in promoting chondrogenesis has been shown in the literature with other stem cells (Sun et al., 2018; Li et al., 2020). Moreover, we observed better macroscopic healing results after 3 months

post-transplantation in animals treated with scaffolds containing rMDSC and TGFβ3 compared to scaffolds with chondrocytes alone. After 6 months, scaffolds with rMDSC and scaffolds containing TGFβ3 had comparable histological and macroscopic results. The findings indicate the TGFβ3 effect on the rMDSC ability to regenerate cartilage tissue for up to 3 months. On the contrary, after 6 months, scaffolds with TGFβ3 had significantly better outcomes than scaffolds alone. The findings suggest that scaffolds with the addition of TGFβ3 may stimulate surrounding host cells for up to 6 months. Various studies proved the beneficial effect of TGFβ3 on cartilage regeneration using different cell types and constructs (Sun et al., 2018; Li et al., 2020; Barati et al., 2020). As our scaffold is well biodegradable, the supplementation of TGFβ3 in the scaffold can promote differentiation and proliferation of remaining tissue chondrocytes in the scenario of cartilage injury (Li et al., 2022). In addition, it is possible that TGFβ3 can engage other types of cells circulating in the synovial fluid including fibroblasts (Denu et al., 2016), MSCs (Barati et al., 2020), or even fat cells (Li et al., 2020) to form new cartilage. At 6 months, a scaffold with TGFβ3 and rMDSCs showed comparable electromechanical,

macroscopic, and histological outcomes to the golden standard scaffold in our study called “control scaffold”—the scaffold embedded with chondrocytes. Chondrocyte-scaffold constructs are already widely applied in cartilage regeneration (Nam et al., 2009; Kon et al., 2011; Anders et al., 2012), having in mind the side effects of stem cells (overgrowth, tumor formation, need for specific conditions for specific tissue formation, etc.). However, the use of chondrocytes has its drawbacks because it can lead to the dedifferentiation of these cells (Mayne et al., 1976; Harrison et al., 2000; Stokes et al., 2001). This can result in further loss of tissue, increase inflammation, and cause progressing loss of the function of the joint. Therefore, another promising technique may be the use of MSCs and growth factors with optimally selected cell count and concentration of growth factor, as well as the selection of biomaterial and its appropriate fabrication to ensure the proper environment for seeded cells. In our study, over the 6-month period, the worsening results of the overall non-cellular groups were determined to show non-endurant properties of the regenerated tissue. Most of the cellular scaffolds demonstrated similar results between the same time-points. Sm and Stm scaffolds had comparable results between 3 and 6 months macroscopically, histologically, and electromechanically, indicating regenerated cartilage tissue-endurant properties over a 3-month period.

In summary, the present study showed the potential of the bilayer PCL scaffold, which was ozonated and loaded with TGF β 3 to stimulate rMDSC differentiation into cartilage tissue *in vitro* and *in vivo* in the rabbit model. This is the first study showing promising results of the combination of different factors (use of two differently prepared layers of the scaffold, ozone treatment, and embedding of stem cells) on articular cartilage regeneration. However, in order to translate the use of our developed scaffold into clinical studies, additional *in vitro* studies should be completed to eliminate the limitations of this scaffold. In addition, more *in vitro* studies should be performed to analyze the selection of the most appropriate concentration of TGF β 3 and the duration when scaffolds are incubated with the growth factor. Repeated *in vivo* studies are required if the results of *in vitro* studies will be significantly inferior/superior to those presented in our experiments. Adding, a longer *in vivo* study with regard to the articular joint function should be accomplished.

Data availability statement

The original contributions presented in the study are included in the article/Supplementary Material; further inquiries can be directed to the corresponding author.

Ethics statement

The animal study was reviewed and approved by the Ethics Committee of the State Food and Veterinary Service (G2-133).

Author contributions

AU—study conceptualization and design; LD, EK, DM, DC, and OB—scaffold production and testing; LJ—rMDSC isolation; MM—rCh isolation; LJ and LA—FACS, microscopy, *in vitro* cell experiments, protein binding, and data analysis; LJ and MM—protein analysis and data analysis; TM, AR, and AU—*in vivo* experiments and data analysis; AP—histology and microscopical *in vivo* tissue analysis; LJ and MM—manuscript drafting; LJ, MM, and AU—manuscript editing. All authors approved the final version of the manuscript.

Funding

This project has received funding from the European Regional Development Fund (project No 01.2.2-LMT-K-718-01-0078) under a grant agreement with the Research Council of Lithuania (LMTLT).

Acknowledgments

The authors kindly thank Prof. J. Kupcinskis' lab for providing access to FACS. They also thank all the patients who contributed to this research. Additionally, they thank Prof. V. Borutaite and her lab for access to the ELISA reader. The authors are grateful to our technician Laurencija Stroliene for all the support and laboratory administration.

Conflict of interest

The authors declare that the research was conducted in the absence of any commercial or financial relationships that could be construed as a potential conflict of interest.

Publisher's note

All claims expressed in this article are solely those of the authors and do not necessarily represent those of their affiliated organizations, or those of the publisher, the editors, and the reviewers. Any product that may be evaluated in this article, or claim that may be made by its manufacturer, is not guaranteed or endorsed by the publisher.

References

- Abpekar, Z., Milan, P. B., Moradi, L., Anjomshoa, M., and Asadpour, S. (2021). Influence of pore sizes in 3D-scaffolds on mechanical properties of scaffolds and survival, distribution, and proliferation of human chondrocytes. *Mech. Adv. Mater. Struct.* doi:10.1080/15376494.2021.1943077
- Anders, S., Goetz, J., Schubert, T., Grifka, J., and Schaumburger, J. (2012). Treatment of deep articular talus lesions by matrix associated autologous chondrocyte implantation - results at five years. *Int. Orthop.* 36 (11), 2279–2285. doi:10.1007/s00264-012-1635-1
- Bae, D. K., Yoon, K. H., and Song, S. J. (2006). Cartilage healing after microfracture in osteoarthritic knees. *Arthrosc. J. Arthrosc. Relat. Surg.* 22 (4), 367–374. doi:10.1016/j.arthro.2006.01.015
- Barati, D., Gegg, C., and Yang, F. (2020). Nanoparticle-mediated TGF- β release from microribbon-based hydrogels accelerates stem cell-based cartilage formation *in vivo*. *Ann. Biomed. Eng.* 48 (7), 1971–1981. doi:10.1007/s10439-020-02522-z
- Borrelli, J., Olson, S. A., Godbout, C., Schemitsch, E. H., Stannard, J. P., and Giannoudis, P. v. (2019). Understanding articular cartilage injury and potential treatments. *J. Orthop. Trauma* 33, S6–S12. doi:10.1097/bot.0000000000001472
- Čamernik, K., Mihalić, A., Mihalić, R., Marolt Presen, D., Janež, A., Trebše, R., et al. (2019). Skeletal-muscle-derived mesenchymal stem/stromal cells from patients with osteoarthritis show superior biological properties compared to bone-derived cells. *Stem Cell Res.* 38, 101465. doi:10.1016/j.scr.2019.101465
- Choukair, D., Hügel, U., Sander, A., Uhlmann, L., and Tönshoff, B. (2014). Inhibition of IGF-I-related intracellular signaling pathways by proinflammatory cytokines in growth plate chondrocytes. *Pediatr. Res.* 76 (3), 245–251. doi:10.1038/pr.2014.84
- Dabasinskaite, L., Krugly, E., Baniukaitiene, O., Ciuzas, D., Martuzevicius, D., Jankauskaite, L., et al. (2022). Design and fabrication method of bi-layered fibrous scaffold for cartilage regeneration. *Biochem. Eng. J.* 182, 108413. doi:10.1016/j.bej.2022.108413
- Dabasinskaite, L., Krugly, E., Baniukaitiene, O., Martuzevicius, D., Ciuzas, D., Jankauskaite, L., et al. (2021). The effect of ozone treatment on the physicochemical properties and biocompatibility of electrospun poly(ϵ)caprolactone scaffolds. *Pharmaceutics* 13 (8), 1288. doi:10.3390/pharmaceutics13081288
- Demoor, M., Ollitrault, D., Gomez-Leduc, T., Bouyoucef, M., Hervieu, M., Fabre, H., et al. (2014). Cartilage tissue engineering: Molecular control of chondrocyte differentiation for proper cartilage matrix reconstruction. *Biochimica Biophysica Acta (BBA) - General Subj.* 1840 (8), 2414–2440. doi:10.1016/j.bbagen.2014.02.030
- Denu, R. A., Nemcek, S., Bloom, D. D., Goodrich, A. D., Kim, J., Mosher, D. F., et al. (2016). Fibroblasts and mesenchymal stromal/stem cells are phenotypically indistinguishable. *Acta Haematol.* 136 (2), 85–97. doi:10.1159/000445096
- Francis, S. L., di Bella, C., Wallace, G. G., and Choong, P. F. M. (2018). Cartilage tissue engineering using stem cells and bioprinting technology—barriers to clinical translation. *Front. Surg.* 5, 70. doi:10.3389/fsurg.2018.00070
- Girão, A. F., Semitela, A., Pereira, A. L., Completo, A., and Marques, P. A. A. P. (2020). Microfabrication of a biomimetic arcade-like electrospun scaffold for cartilage tissue engineering applications. *J. Mat. Sci. Mat. Med.* 31 (8), 69–9. doi:10.1007/s10856-020-06407-4
- Gomez-Salazar, M., Gonzalez-Galofre, Z. N., Casamitjana, J., Crisan, M., James, A. W., and Péault, B. (2020). Five decades later, are mesenchymal stem cells still relevant? *Front. Bioeng. Biotechnol.* 8, 148. doi:10.3389/fbioe.2020.00148
- Grafe, I., Alexander, S., Peterson, J. R., Snider, T. N., Levi, B., Lee, B., et al. (2018). TGF- β family signaling in mesenchymal differentiation. *Cold Spring Harb. Perspect. Biol.* 10 (5), a022202. doi:10.1101/cshperspect.a022202
- Harrison, P. E., Ashton, I. K., Johnson, W. E. B., Turner, S. L., Richardson, J. B., and Ashton, B. A. (2000). The *in vitro* growth of human chondrocytes. *Cell Tissue Bank.* 1 (4), 255–260. doi:10.1023/a:1010131729208
- Hunziker, E. B., Quinn, T. M., and Häuselmann, H. J. (2002). Quantitative structural organization of normal adult human articular cartilage. *Osteoarthr. Cartil.* 10 (7), 564–572. doi:10.1053/joca.2002.0814
- Jankauskaite, L., Malinauskas, M., Aukstikalne, L., Dabasinskaite, L., Rimkunas, A., Mickevicius, T., et al. (2022). Functionalized electrospun scaffold-human-muscle-derived stem cell construct promotes *in vivo* neocartilage formation. *Polym. (Basel)* 14 (12), 2498. doi:10.3390/polym14122498
- Jelodari, S., Ebrahimi Sadrabadi, A., Zarei, F., Jahangir, S., Azami, M., Sheykhasan, M., et al. (2022). New insights into cartilage tissue engineering: Improvement of tissue-scaffold integration to enhance cartilage regeneration. *BioMed Res. Int.* 2022, 1–13. doi:10.1155/2022/7638245
- Kon, E., Filardo, G., Berruto, M., Benazzo, F., Zanon, G., della Villa, S., et al. (2011). Articular cartilage treatment in high-level male soccer players: A prospective comparative study of arthroscopic second-generation autologous chondrocyte implantation versus microfracture. *Am. J. Sports Med.* 39 (12), 2549–2557. doi:10.1177/0363546511420688
- Lavasani, M., Lu, A., Thompson, S. D., Robbins, P. D., Huard, J., and Niedernhofer, L. J. (2013). Isolation of muscle-derived stem/progenitor cells based on adhesion characteristics to collagen-coated surfaces. *Methods Mol. Biol.* 976, 53–65. doi:10.1007/978-1-62703-317-6_5
- Li, D., Ma, X., and Zhao, T. (2020). Mechanism of TGF- β 3 promoting chondrogenesis in human fat stem cells. *Biochem. Biophys. Res. Commun.* 530 (4), 725–731. doi:10.1016/j.bbrc.2020.06.147
- Li, M., Yin, H., Yan, Z., Li, H., Wu, J., Wang, Y., et al. (2022). The immune microenvironment in cartilage injury and repair. *Acta Biomater.* 140, 23–42. doi:10.1016/j.actbio.2021.12.006
- Makris, E. A., Gomoll, A. H., Malizos, K. N., Hu, J. C., and Athanasiou, K. A. (2015). Repair and tissue engineering techniques for articular cartilage. *Nat. Rev. Rheumatol.* 11 (1), 21–34. doi:10.1038/nrrheum.2014.157
- Mayne, R., Vail, M. S., Mayne, P. M., and Miller, E. J. (1976). Changes in type of collagen synthesized as clones of chick chondrocytes grow and eventually lose division capacity. *Proc. Natl. Acad. Sci. U. S. A.* 73 (5), 1674–1678. doi:10.1073/pnas.73.5.1674
- Mickevicius, T., Pockevicius, A., Kucinskas, A., Gudas, R., MacLulaitis, J., Noreikaite, A., et al. (2015). Impact of storage conditions on electromechanical, histological and histochemical properties of osteochondral allografts. *BMC Musculoskelet. Disord.* 16 (1), 314. doi:10.1186/s12891-015-0776-y
- Mohammadinejad, R., Kumar, A., Ranjbar-Mohammadi, M., Ashrafzadeh, M., Han, S. S., Khang, G., et al. (2020). Recent advances in natural gum-based biomaterials for tissue engineering and regenerative medicine: A review. *Polym. (Basel)* 12 (1), 176. doi:10.3390/polym12010176
- Music, E., Klein, T. J., Lott, W. B., and Doran, M. R. (2020). Transforming growth factor-beta stimulates human bone marrow-derived mesenchymal stem/stromal cell chondrogenesis more so than kartogenin. *Sci. Rep.* 10 (1), 8340. doi:10.1038/s41598-020-65283-8
- Nam, E. K., Ferkel, R. D., and Applegate, G. R. (2009). Autologous chondrocyte implantation of the ankle: A 2- to 5-year follow-up. *Am. J. Sports Med.* 37 (2), 274–284. doi:10.1177/0363546508325670
- Pearson, R. G., Kurien, T., Shu, K. S. S., and Scammell, B. E. (2011). Histopathology for grading systems for characterisation of human knee osteoarthritis—reproducibility, variability, reliability, correlation, and validity. *Osteoarthr. Cartil.* 19 (3), 324–331. doi:10.1016/j.joca.2010.12.005
- Pittenger, M. F., Discher, D. E., Péault, B. M., Phinney, D. G., Hare, J. M., and Caplan, A. I. (2019). Mesenchymal stem cell perspective: Cell biology to clinical progress. *npj Regen. Med.* 4 (1), 22–15. doi:10.1038/s41536-019-0083-6
- Qin, X., Wu, Y., Liu, S., Yang, L., Yuan, H., Cai, S., et al. (2022). Surface modification of polycaprolactone scaffold with improved biocompatibility and controlled growth factor release for enhanced stem cell differentiation. *Front. Bioeng. Biotechnol.* 9, 802311. doi:10.3389/fbioe.2021.802311
- Redigueri, C. F., de Bank, P. A., Zanin, M. H. A., Leo, P., Cerize, N. N. P., de Oliveira, A. M., et al. (2017). The effect of ozone gas sterilization on the properties and cell compatibility of electrospun polycaprolactone scaffolds. *J. Biomaterials Sci. Polym. Ed.* 28 (16), 1918–1934. doi:10.1080/09205063.2017.1358549
- Samsudin, N., Hashim, Y. Z. H. Y., Arifin, M. A., Mel, M., Salleh, H. M., Sopyan, I., et al. (2017). Optimization of ultraviolet ozone treatment process for improvement of polycaprolactone (PCL) microcarrier performance. *Cytotechnology* 69 (4), 601–616. doi:10.1007/s10616-017-0071-x
- Samsudin, N., Hashim, Y. Z. H., Arifin, M. A., Mel, M., Mohd Salleh, H., Sopyan, I., et al. (2018). Surface modification of Polycaprolactone (PCL) microcarrier for performance improvement of human skin fibroblast cell culture. *IOP Conf. Ser. Mat. Sci. Eng.* 290 (1), 012016. doi:10.1088/1757-899x/290/1/012016
- Sokolove, J., and Lepus, C. M. (2013). Role of inflammation in the pathogenesis of osteoarthritis: Latest findings and interpretations. *Ther. Adv. Musculoskelet. Dis.* 5 (2), 77–94. doi:10.1177/1759720x12467868
- Sousa, I., Mendes, A., Pereira, R. F., and Bártolo, P. J. (2014). Collagen surface modified poly(ϵ -caprolactone) scaffolds with improved hydrophilicity and cell adhesion properties. *Mater. Lett.* 134, 263–267. doi:10.1016/j.matlet.2014.06.132

Stewart, A. G., Thomas, B., and Koff, J. (2018). TGF- β : Master regulator of inflammation and fibrosis. *Respirology* 23 (12), 1096–1097. doi:10.1111/resp.13415

Stokes, D. G., Liu, G., Dharmavaram, R., Hawkins, D., Piera-Velazquez, S., and Jimenez, S. A. (2001). Regulation of type-II collagen gene expression during human chondrocyte de-differentiation and recovery of chondrocyte-specific phenotype in culture involves Sry-type high-mobility-group box (SOX) transcription factors. *Biochem. J.* 360 (2), 461–470. doi:10.1042/bj3600461

Sun, Q., Zhang, L., Xu, T., Ying, J., Xia, B., Jing, H., et al. (2018). Combined use of adipose derived stem cells and TGF- β 3 microspheres promotes articular cartilage regeneration *in vivo*. *Biotech. Histochem.* 93 (3), 168–176. doi:10.1080/10520295.2017.1401663

Theodoridis, K., Aggelidou, E., Manthou, M., Demiri, E., Bakopoulou, A., and Kritis, A. (2019). Assessment of cartilage regeneration on 3D collagen-polycaprolactone scaffolds: Evaluation of growth media in static and in perfusion bioreactor dynamic culture. *Colloids Surfaces B Biointerfaces* 183, 110403. doi:10.1016/j.colsurfb.2019.110403

Wang, W., Rigueur, D., and Lyons, K. M. (2014). TGF β signaling in cartilage development and maintenance. *Birth Defect. Res. C* 102 (1), 37–51. doi:10.1002/bdrc.21058

Yoshimura, A., Wakabayashi, Y., and Mori, T. (2010). Cellular and molecular basis for the regulation of inflammation by TGF- β . *J. Biochem.* 147 (6), 781–792. doi:10.1093/jb/mvq043